ELSEVIER

Synthetic Metals 122 (2001) 387–393

SYNTHETIC METALS

www.elsevier.com/locate/synmet

Energy transfer from poly(2-carboxyphenylene-1,4-diyl) to poly(*p*-phenylene vinylene) in bilayer films and its effects on luminescent properties

Horng-Long Cheng, King-Fu Lin*

Institute of Materials Science and Engineering, National Taiwan University, Taipei 10617, Taiwan, ROC

Received 28 April 2000; received in revised form 28 July 2000; accepted 3 August 2000

Abstract

Luminescent properties of poly(*p*-phenylenevinylene) (PPV) in bilayer films were found significantly enhanced by energy transfer from poly(2-carboxyphenylene-1,4-diyl) (PCPD) to PPV prepared by alternatively spin-coating the poly(xylylene tetrahydrothiophenium chloride) (PXT, dubbed as PPV-precursor) aqueous solution and PCPD pyridine solution followed by heat treatments. The energy transfer process, as verified by the photoluminescent excitation (PLE) spectroscopy and the analysis of time-resolved photoluminescence (PL) decays, was attributed to the chemical interlocking between two polymers in the interfacial region. Accordingly, the efficiency of energy transfer from PCPD to PPV was calculated. Consequently, the (glass)PPV/PCPD configuration exhibited higher energy transfer efficiency than the (glass)PCPD/PPV, resulting in higher PL and electroluminescent (EL) quantum efficiencies. Besides, the improved EL emission of indium-tin-oxide (ITO)/PPV/PCPD/Al device was attributed to the energy barrier in the PPV/PCPD interfacial region, which trapped the majority carriers, holes, to form the excitons in situ, that decayed radiatively.

Keywords: Poly(*p*-phenylenevinylene); Poly(*p*-phenylene); Energy transfer; Photoluminescence; Electroluminescence

1. Introduction

Polymeric light-emitting devices (PLEDs) have became a very active research area since discovery of the electroluminescent (EL) properties of poly(*p*-phenylene vinylene) (PPV) [1]. PPV is a yellowish-green emissive polymer, which is insoluble and intractable but can be prepared via a soluble precursor route to obtain a thin film [1]. However, the quantum efficiency of PPV in EL emission is rather low. Efforts to achieve a higher luminescent efficiency through innovation of emission mechanism have been one of the approaches for the development of PLEDs [2–7].

Energy transfer is an important photophysical process. A spectral overlap between the absorption of the acceptor and the emission of the donor and a proper host-guest spacing are required for the efficient energy transfer [4,8]. Recent researchers [4–7] have shown that it is possible to obtain a complete internal transfer of excitations between host-guest (or donor-acceptor) polymeric pairs, enhancing the photoluminescence (PL) and EL emissions.

Poly(2-carboxyphenylene-1,4-diyl) (PCPD) is a conjugated polymer with blue emission peaked at 420 nm, which is within the optical absorption region of PPV [9]. A good spectral overlap between the emission of PCPD and the absorption of PPV was believed to lead to an efficient energy transfer if they were miscible. Unfortunately, a solution mixing of PPV precursor (containing tetrahydrothiophenium cationic groups) and PCPD (containing carboxylic anionic groups) was not obtained because of the formation of a polyion complex. Thus, in this study, the PPV/PCPD and PCPD/PPV bilayer films were prepared by alternatively spin-coating the PPV precursor aqueous solution and the PCPD pyridine solution with following heat treatment. An arrangement of adjacent positive and negative polyion layers resulted in better interpenetrating between two polymers (see Fig. 1). Consequently, significant energy transfer from PCPD to PPV was observed, therefore enhancing the PL and EL emissions from PPV. In this paper, we report the energy transfer phenomenon from PCPD toward PPV and calculate the energy transfer efficiency in terms of the sample configurations. Besides, the effect of energy transfer on EL emission of bilayer films will also be discussed.

* Corresponding author. Tel.: +886-2-2392-8290; fax: +886-2-2363-4562.
E-mail address: kflin@ccms.ntu.edu.tw (K.-F. Lin).

0379-6779/01/$ – see front matter
PII: S0379-6779(00)00395-7

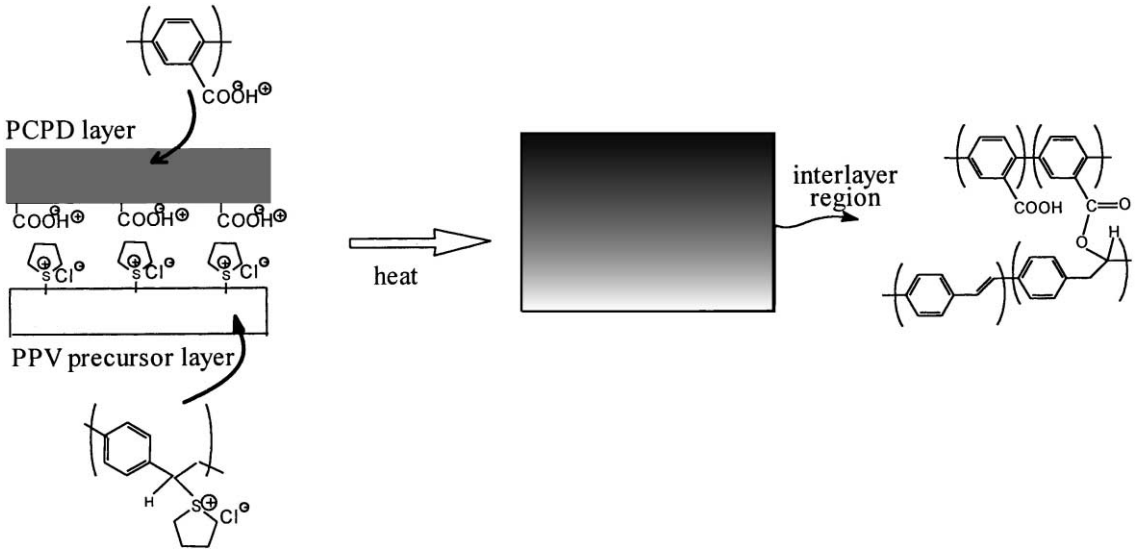

Fig. 1. Schematic representation of formation of PPV/PCPD bilayer film. The gradation of tone in the bilayer film indicates the expected mutual interpenetrating between two polymers in the interfacial region.

2. Experimental

2.1. Materials

Poly(xylylene tetrahydrothiophenium chloride) (PXT, also dubbed as PPV precursor) with a weight average molecular weight (M_w) of 1.2×10^6 and a molecular weight dispersity of 3.2 relative to the polystyrene standards (measured by gel permeation chromatography), was prepared via a modified sulfonium precursor route [10,11]. The detailed description has been reported elsewhere [12,13]. The PCPD with a M_w of 1.3×10^3 and a dispersity of 1.75 was synthesized by the Chaturvedi method [14]. The prepared PCPD was insoluble in most of the hydrocarbon solvents, but soluble in basic solvents such as pyridine and quinoline.

2.2. Fabrication of light-emitting films and devices

Neat PPV film was prepared by spin coating the PXT aqueous solution (~0.25 wt.%) onto an indium-tin-oxide (ITO)-coated glass plates (20 Ω/sq, Merck Co.) followed by heat treatment at 180°C for 2 h (in vacuum $<10^{-5}$ Torr). Neat PCPD film was prepared by spin coating its pyridine solution (~15 mg/ml) onto an ITO-coated glass plate and the pyridine solvent removed at 180°C under high vacuum. The two bilayer films, (glass/ITO)PPV/PCPD and (glass/ITO)PCPD/PPV, were fabricated by the following procedure: in the beginning, PXT in aqueous solution or PCPD in pyridine solution was spin-coated onto the ITO-coated glass plates; after drying, the second layer was spin-coated from their corresponding solutions over the previous layer to prepare the (glass/ITO)PXT/PCPD and (glass/ITO)PCPD/PXT bilayer films; the bilayer films were then heat-treated at 180°C at vacuum $<10^{-5}$ Torr for 2 h to give the final (glass/ITO)PPV/PCPD or (glass/ITO)PCPD/PPV configurations. After heat treatment, the bilayer films appeared to be homogeneous and transparent. The thickness of each layers was controlled at $\sim 50 \pm 5$ nm by adjusting the spin-coating speed and solution concentrations. All samples have a thickness of 100 ± 10 nm as measured by a surface profilometer (Dektek Co., Model 3030).

The PLED devices used in this study, typically consisting of an ITO on glass substrate as a hole-injecting electrode, a polymer film, and an evaporated Al metal acting as an electron-injecting electrode. Evaporation of the Al metal electrode was performed by using a thermal evaporator (JEOL Co., Model JEE-4C). The coated Al electrode should be uniform with thickness ranging from 1500 to 2000 Å. The active areas of each device for emission were 3 mm^2.

2.3. Characterization

Infrared spectra of the polymer films (removed from the coated glass substrates) were recorded on a Jasco 300E model FTIR spectrometer. The UV–VIS absorption spectra were recorded on a Jasco-555 model spectrometer. PL and photoluminescence excitation (PLE) spectra of the films were recorded on a Jasco FR-777 spectrofluorometer. The current–voltage (*I–V*) characteristics of the devices were measured by a Keithley 2400 model electrometer, where the concurrent EL intensities were recorded by using a calibrated photometer (International Light, Inc., model IL1400A). Thus, the external quantum yield (photons per electron) was determined by using the measured EL intensity under the applied current. EL spectra of devices were recorded on a Jasco FR-777 spectrofluorometer. Time-resolved fluorescence of the specimens in a closed cycle cryostat under vacuum ($<10^{-5}$ Torr) at room temperature

was recorded by a time-correlated single photon counting apparatus with a time resolution of ~80 ps. The excitation was from the triplet of Ti:Sapphire laser at a wavelength of 290 nm. The excitation power was <1 mW. Cyclic voltammograms of the polymer films cast on the ITO substrate were recorded against a Ag/AgCl reference electrode by using a conventional three-electrode cell in an acetonitrile/0.1 M tetrabutylammonium tetrafluoroborate solution. A platinum plate was used as a counter electrode.

3. Results

Fig. 2 shows the infrared spectra of PPV, PCPD, PPV/PCPD, and PCPD/PPV films, respectively. The chemical interlocking at the interface between two polymers in bilayer films were suggested by the following: the band at 965 cm^{-1} contributed by the bending vibration of trans-vinylene C–H out of plane mode from PPV was shifted to lower frequencies. Similar shifting was also reported for the PPV chains with shorter conjugated length [13,15]. In addition, the band at 1228 cm^{-1} contributed by the asymmetrical and symmetrical C–O stretching vibrations from PCPD shifted to higher frequencies owing to the formation of C–O–C linkage.

Fig. 3 shows the normalized absorption spectra of the bilayer films in comparison with the neat PPV and PCPD films. The absorptions of the PPV and PCPD films have the onset wavelengths (λ_{onset}) at 525 nm (2.36 eV) and 372 nm (3.32 eV), respectively, and the maximum (λ_{max}) at 422 and 322 nm, respectively. In general, the absorptions of the bilayer films have a similar pattern as the sum of two individual absorptions. However, by scrupulous examination, the bandgaps ($E_g = hv/\lambda_{onset}$) of PCPD/PPV and PPV/PCPD are about 2.39 and 2.51 eV, respectively, larger than that of the neat PPV (2.36 eV). The absorption of PPV in bilayer films is blue-shifted compared to the neat PPV, indicating that the PPV in bilayer films has less extent of conjugations, which is in agreement with the results obtained from the infrared spectroscopy. The lower absorption intensity of PPV in bilayer films compared to the neat PPV might also be due to the less extent of conjugation, since they had been normalized to the same absorption intensity of neat PCPD with a thickness of 100 nm (see Fig. 3).

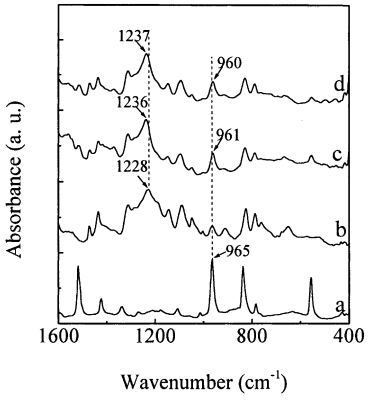

Fig. 2. Infrared spectrum of (a) PPV, (b) PCPD, (c) PCPD/PPV, and (d) PPV/PCPD films.

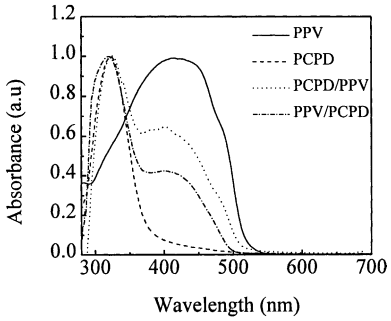

Fig. 3. Absorption spectra of PPV, PCPD, PCPD/PPV, and PPV/PCPD films. Note: spectra of the PCPD/PPV and PPV/PCPD bilayer films have been normalized to the maximum absorption of neat PCPD.

Fig. 4 shows the PL spectra of PPV, PCPD, and the bilayer films, respectively, upon excitation at a wavelength of 290 nm. The PL spectrum of neat PPV film has two major emission peaks at 520 and 550 nm, which have been assigned to the 0–0 and 0–1 transition bands, respectively [16,17]. The PL spectrum of PCPD film has a strong blue emission peak at 420 nm. Interestingly, the PL spectra of bilayer films exhibit a major emission from PPV and a weak emission from PCPD. The major emission peaks of PCPD/PPV and PPV/PCPD films have the intensities of 2.58 and 3.64 times that of the neat PPV film, respectively, with slight blue shift. Again, the blue shift is owing to the less extent of conjugation in PPV chains.

Fig. 5 shows the EL spectra of ITO/PPV/Al, ITO/PCPD/PPV/Al, ITO/PPV/PCPD/Al light emitting diodes (LEDs) devices, respectively, with ITO as an anode and Al as a cathode. The EL spectra of PCPD/PPV and PPV/PCPD bilayer films are basically similar to that of the PPV but with blue shift by 20–40 nm. In contrast to PL counterparts, we have not observed any emission from PCPD in the EL spectra of bilayer films. The blue shifts in the PL and EL are in agreement with the blue shifts in the absorption

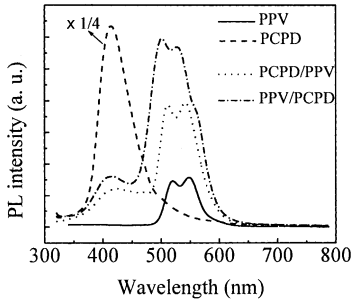

Fig. 4. PL spectra of PPV, PCPD, PCPD/PPV, and PPV/PCPD films excited at 290 nm. Note: the PL intensity of neat PCPD is four times more than shown.

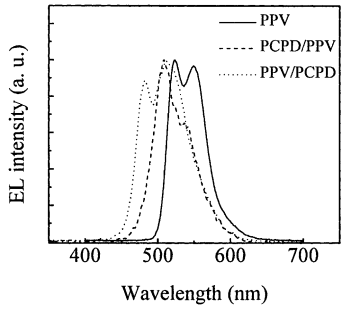

Fig. 5. EL spectra of ITO/PPV/Al, ITO/PCPD/PPV/Al, and ITO/PPV/PCPD/Al devices. Note: spectra have been normalized to the maximum.

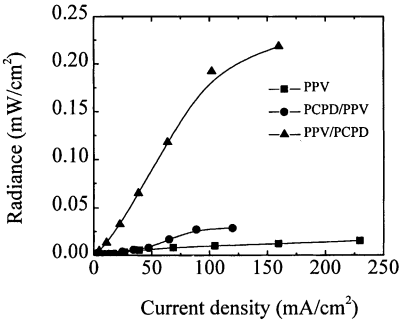

Fig. 7. Current density–radiance characteristics of ITO/PPV/Al (■), ITO/PCPD/PPV/Al (●), and ITO/PPV/PCPD/Al (▲) devices.

(PPV/PCPD is bluer than PCPD/PPV, which in turn is bluer than PPV).

Fig. 6a shows the current density of ITO/PPV/Al, ITO/PCPD/PPV/Al and ITO/PPV/PCPD/Al LED devices, respectively, as a function of the applied voltages. Their concurrent EL intensities versus voltages were plotted in Fig. 6b. As seen in the figure, the turn-on voltage (V_{on}) of the bilayer film devices is significantly higher than that of the neat PPV.

Fig. 7 shows the plot of EL radiance versus the current density obtained from the rearrangements of the data shown in Fig. 6a and b. As seen in the figure, the radiance of the bilayer film devices is stronger than that of the neat PPV based on the same current density. The maximum EL light outputs of ITO/PCPD/PPV/Al and ITO/PPV/PCPD/Al devices were about 2.4 and 18.2 times that of the ITO/PPV/Al, respectively. The maximal external quantum yields of EL (photons/electron) of ITO/PCPD/PPV/Al and ITO/PPV/PCPD/Al devices were 1.4×10^{-2}% at 11 V and 8.3×10^{-2}% at 9.5 V, which are also higher than that of PPV (5.3×10^{-3}% at 5.5 V).

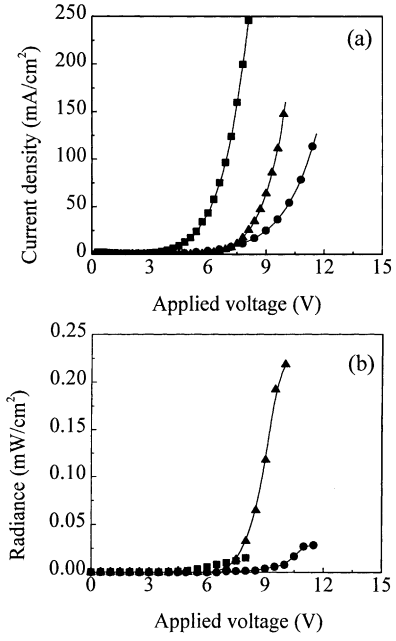

Fig. 6. (a) Current density–voltage and (b) radiance–voltage characteristics of ITO/PPV/Al (■), ITO/PCPD/PPV/Al (●), and ITO/PPV/PCPD/Al (▲) devices.

4. Discussion

4.1. Energy transfer phenomenon

The increase of PL intensity of PPV in bilayer films compared to the neat PPV shown in Fig. 4 was considered to mostly result from the energy transfer from PCPD to PPV. To obtain concrete evidence, we have looked into the PLE and time-resolved PL spectroscopies. Fig. 8a shows the PLE spectra of neat PPV and PCPD contributing to their emissions at wavelengths of 550 and 420 nm, respectively. The PLE spectrum of PPV is broadly flat after the onset of the polymer absorption at 2.47 eV, as previously reported [18]. The PLE spectrum of PCPD is very similar to its UV–VIS absorption spectrum shown in Fig. 3. Fig. 8b and c show the PLE spectra of PCPD/PPV and PPV/PCPD bilayer films, respectively contributing to their maximum emissions from PPV at $\lambda_{em} = 542$ nm and from PCPD at $\lambda_{em} = 420$ nm (see Fig. 4). As shown in the figures, the PLE of bilayer films for the PPV emissions at $\lambda_{em} = 542$ nm is not only from PPV but also from PCPD. However, the intensity of PLE for the PCPD emissions in bilayer films at $\lambda_{em} = 420$ nm is much smaller compared to that of the neat PCPD. Such behaviors may be explained by the following. The absorption of light (absorption energy $> E_g$), promotes the π-electrons of PCPD-chains to the singlet excited state, which rapidly decay to the first singlet excited state by internal conversion. In this stage, some of the excited π-electrons nonradiatively transfer their energy to PPV chains by promoting the π-electrons of PPV to the singlet excited sate, which also rapidly decay to the first singlet excited state by internal conversion. Finally, some of the excited π-electrons in PPV chains drop to the ground state with radiation.

Direct evidences of energy transfer from PCPD to PPV in bilayer films are obtained by time-resolved PL measurements. Fig. 9 shows the picosecond time-resolved PL decay

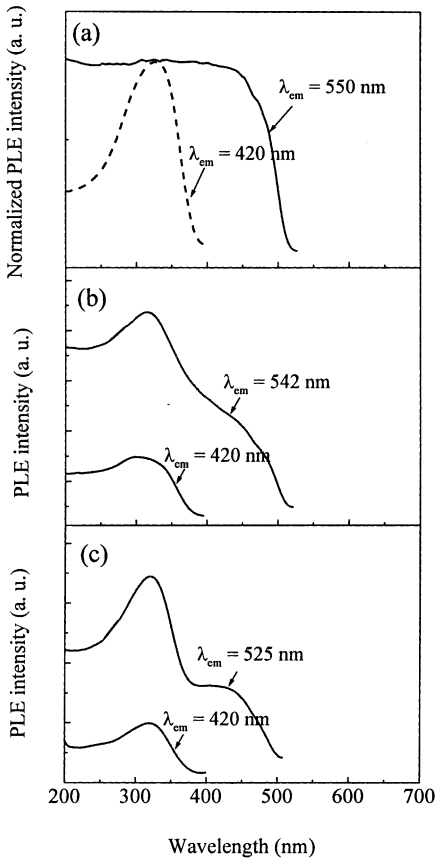

Fig. 8. (a) PLE spectra of PPV and PCPD films contributing to the maximum emission at $\lambda_{em} = 550$ and 420 nm, respectively; (b) PLE spectra of PCPD/PPV bilayer film at $\lambda_{em} = 542$ and 420 nm; and (c) PLE spectra of PPV/PCPD bilayer film at $\lambda_{em} = 525$ and 420 nm.

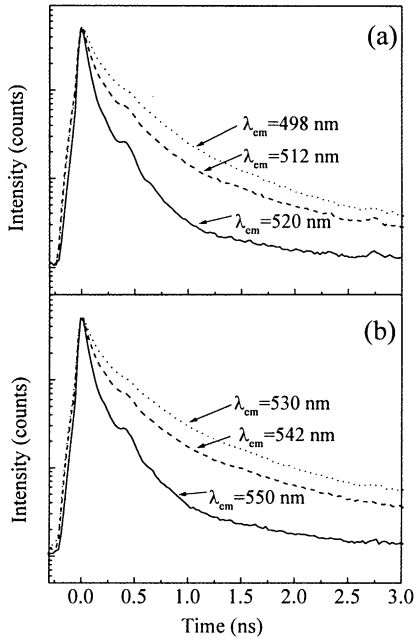

Fig. 9. Time-resolved PL of PPV (solid line), PCPD/PPV (– – –), and PPV/PCPD (· · ·) at a pump wavelength of 290 nm, collected at (a) 0–0 and (b) 0–1 transition bands (as indicated by λ_{em}) of PPV, respectively. Note: the curves have been normalized to the same peak intensity.

profiles of PPV in single layer and bilayer films pumped by pulse at a wavelength of 290 nm at room temperature. The decay dynamics were monitored at two wavelengths corresponding to the 0–0 and 0–1 transition bands of PPV, respectively. The decay profiles cannot be described with simple exponential decay, similar to previously reports for the decay of PPV in solid state [19–24]. For such non-exponential decays, it is not straightforward to measure the lifetime of the decay. However, the lifetime may be considered to be the average time period a chromophore spends in the excited state. Thus, the average lifetime $\langle\tau\rangle$ determined from the area under the decay curve is given by [25][1]

$$\langle\tau\rangle = \frac{\int_0^\infty tI(t)\,\mathrm{d}t}{\int_0^\infty I(t)\,\mathrm{d}t} \tag{1}$$

where $I(t)$ is the PL intensity at time t following excitation. The results are shown in Table 1. The increase in lifetime for PPV in the bilayer films is rather large. As the Förster transfer process is fairly quick (10–20 ps), the increase in the lifetimes of over 100 ps must have some other origin. The process of absorption of the PCPD emission and subsequent re-emission might be able to explain this increase in lifetime.

The PL decays of PCPD in single layer and bilayer films were also monitored at 420 nm as shown in Fig. 10, the wavelength that corresponds to the PCPD emission maximum. Similar to the PPV emission decay, the decay dynamics of PCPD represent a non-exponential decay so that we used Eq. (1) to calculate the average lifetime. The results were also included in Table 1. The decrease in lifetime (τ) of PCPD in bilayer films compared to the neat PCPD (τ_1) is the clearest evidence of a parallel decay process, such as Förster transfer. The lifetimes of this parallel process might be calculated using the equation

$$\frac{1}{\tau} = \frac{1}{\tau_1} + \frac{1}{\tau_2} \tag{2}$$

where τ_2 is the lifetime of PCPD emission through the Förster transfer process. The calculated τ_2 are quite long (1365 and 912 ps for PCPD/PPV and PPV/PCPD bilayer films, respectively). This could be due to the fact that Förster transfer does not take place in the bulk of the material but is possible only close to the interface.

The efficiency of energy transfer (φ_{ET}) can be calculated from the intensity of the donor (PCPD) in the presence (I_{da}) and absence (I_d) of the acceptor (PPV) by using the following equation [26]:

$$\varphi_{ET} = 1 - \frac{I_{da}}{I_d} = 1 - \frac{\int_0^\infty I_{da}(t)\,\mathrm{d}t}{\int_0^\infty I_d(t)\,\mathrm{d}t} \tag{3}$$

where $I_{da}(t)$ and $I_d(t)$ are the PL decay functions of donor in the presence and absence of acceptor, respectively. Accordingly, the estimated φ_{ET} for PCPD/PPV and PPV/PCPD

[1] It should be noted that the time distribution of the pulse was ignored.

Table 1
Average lifetimes $\langle\tau\rangle$ at the indicated emission wavelengths measured from the PL decay dynamics of PPV, PCPD, PCPD/PPV, and PPV/PCPD at a pump wavelength of 290 nm

Samples	$\langle\tau\rangle$ from PPV emission (ps)		$\langle\tau\rangle$ from PCPD emission at 420 nm (ps)
	0–0 Transition band[a]	0–1 Transition band[b]	
PPV	230	249	–
PCPD	–	–	517
PCPD/PPV	323	383	375
PPV/PCPD	399	484	330

[a] The wavelengths, λ_{em} have been indicated in Fig. 9a.
[b] The wavelengths, λ_{em} have been indicated in Fig. 9b.

bilayer films are 27 and 36%, respectively. However, the Förster transfer efficiency has been suggested to directly relate to the distance (r) between the donors and acceptors using [26]

$$\phi_{ET} = \frac{R_0^6}{R_0^6 + r^6} \quad (4)$$

where R_0 is the Förster distance defined as the distance at which the transfer rate is equal to the decay rate of the donor in the absence of acceptor. As a result, the effective distance between the donors and acceptors for energy transfer was usually reported up to 50 Å [26]. Above that distance, the transfer efficiency decreases rapidly as suggested by Eq. (4). Thus, since the layer thickness in bilayer films is ~500 Å, the majority of Förster energy transfer between PPV and PCPD should occur in the chemically interlocked interfacial region. The higher transfer efficiency of PPV/PCPD bilayer over PCPD/PPV might be attributed to the higher extent of chemical reaction between two polymers as indicated by their FTIR results shown in Fig. 2. However, owing to the fact that the layer thickness in bilayer films is much larger than the Förster transfer range, the process that the emission from PCPD is absorbed in PPV followed by emission from PPV should also contribute to the higher energy transfer rate between PCPD and PPV.

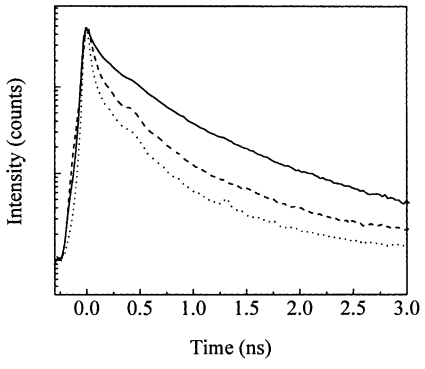

Fig. 10. Time-resolved PL of PCPD (solid line), PCPD/PPV (– – –), and PPV/PCPD (· · ·) at a pump wavelength of 290 nm, collected at 420 nm, the maximum emission wavelength of PCPD. Note: the curves have been normalized to the same peak intensity.

4.2. Electroluminescence

In PLED, the luminescence is obtained from the recombination of electrons (injected from the Al cathode) and holes (injected from the ITO anode) in the polymer thin films to form the singlet excitons, that lose energy by radiation. The energy band diagrams of the bilayer devices are schematically shown in Fig. 11. The lowest unoccupied molecular orbital levels (LUMO) and highest occupied molecular orbital levels (HOMO) of PPV and PCPD were determined from the onset potentials for the reduction and oxidation processes in their cyclic voltammetry data plus 4.4 eV for correction [27,28]. The work functions of ITO and Al are obtained from the literature [29]. Because the Schottky energy barriers in the ITO/PPV and ITO/PCPD contacts of anode are much smaller than those in the Al/PPV and Al/PCPD contacts of cathode, the energy barriers to inject holes from ITO should control the I–V characteristics according to

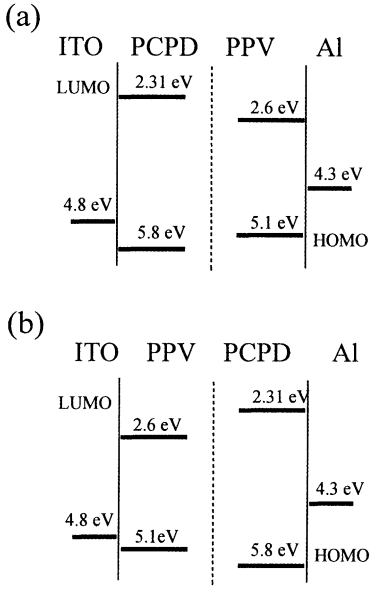

Fig. 11. Energy band diagrams of (a) ITO/PCPD/PPV/Al and (b) ITO/PCPD/PPV/Al devices. The dashed line indicates the undefined interfacial region.

Parker [29]. It explains why the ITO/PCPD/PPV/Al device has higher operating voltage than the ITO/PPV/PCPD/Al as shown in Fig. 6 and holes should be the majority carrier in the PLEDs under study.

For the ITO/PPV/PCPD/Al device, the electrons are trapped by the holes accumulated at the interface of the bilayer due to the energy barrier between PPV and PCPD. This trapping takes place close to the interface as the mobility lifetime product (given by $\mu\tau$ as defined by Antoniadis et al. [30]) for the electrons is rather small ($\sim$1 nm). Thus, all the excitons are formed near the interface and are mostly limited to PPV due to the hole trapping at the barrier. Besides, since the interfacial region consists of the chemically interlocked PPV/PCPD chains as indicated by the FTIR spectra shown in Fig. 2, if the formed excitons resided in the PCPD chains, they would have more chances to undergo the energy transfer to PPV. Conversely, if the excitons resided in the PPV chains, they would have less chance to be quenched by energy transfer because of the higher energy bandgaps of surrounding PCPD polymer chains. As a result, only emission from PPV with high EL quantum efficiency was observed.

As to the ITO/PCPD/PPV/Al device, the electrons face a barrier at the interface. The holes have a much larger mobility lifetime product so that the excitons can be formed farther away from the interface (leading to less efficient Förster transfer). The excitons are predominantly formed in PPV due to the energy barrier faced by the electrons. As a result, their formed excitons have much less concentration than those of the ITO/PPV/PCPD/Al device. Nevertheless, its EL quantum efficiency is still higher than that of the neat PPV.

5. Conclusions

The mutual interpenetrating and chemical interlocked interfaces in the designed PPV/PCPD and PCPD/PPV bilayer films provided the specific region for the energy transfer from PCPD to PPV that increased the PL and EL emissions of PPV. The significantly higher EL quantum yield for the ITO/PPV/PCPD/Al device compared to the ITO/PCPD/PPV/Al was attributed to the energy barrier in the PPV/PCPD interfacial region that trapped the majority carriers, holes. The trapped holes caught the electrons to form the excitons in situ. If the formed excitons resided in the PCPD chains, they have more chances to transfer their energy to PPV. If they resided in the PPV chains, they had less chance to be quenched. As a result, only EL emission from PPV was observed.

Acknowledgements

The authors would like to acknowledge the financial support of the National Science Council in Taiwan, Republic of China through Grant NSC 87-2216-E-002-01. We also thank Prof. W.S. Fann and Dr. J.H. Hsu, Institute of Atomic and Molecular Sciences, Academia Sinica, for the technical assistance with the time-resolved photoluminescence measurements.

References

[1] J.H. Burroughes, D.D.C. Bradley, A.R. Brown, R.N. Marks, K. Mackay, R.H. Friend, P.L. Burn, A.B. Holmes, Nature 347 (1990) 539.
[2] S.A. Jenekhe, J.A. Osaheni, Science 265 (1994) 539.
[3] N. Tessler, N.T. Harrison, R.H. Friend, Adv. Mater. 10 (1998) 64.
[4] R. Gupta, M. Stevenson, A. Dogariu, M.D. McGehee, J.Y. Park, V. Srdanov, A.J. Heeger, H. Wang, Appl. Phys. Lett. 73 (1998) 24.
[5] S. Tasch, J.W. List, C. Hochfilzer, H. Leising, P. Schlichting, U. Rohr, Y. Geerts, U. Scherf, K. Müllen, Phys. Rev. B 56 (1997) 4479.
[6] I.N. Kang, D.H. Hwang, H.K. Shim, T. Zyung, J.J. Kim, Macromolecules 29 (1996) 165.
[7] J.I. Lee, I.N. Kang, D.H. Hwang, H.K. Shim, Chem. Mater. 8 (1996) 1925.
[8] R.C. Powell, Z.G. Soos, J. Lumin. 11 (1975) 1.
[9] H.L. Cheng, K.F. Lin, in: Proceedings of International Conference on Science and Technologies of Advanced Polymers, ICAP99-Yamagata, Yamagata, Japan, 1999, p. 126.
[10] R.A. Wessling, J. Polym. Sci., Polym. Symp. 72 (1985) 55.
[11] R.W. Lenz, C.C. Han, J. Stenger-Smith, F.E. Karasz, J. Polym. Sci.: Polym. Chem. 26 (1988) 3241.
[12] K.F. Lin, L.K. Chang, H.L. Cheng, in: J. Simpson, I. Khan (Eds.), Field Responsive Polymers, ACS symposium Series 726, American Chemical Society, Washington, DC, 1999 (Chapter 5).
[13] H.L. Cheng, K.F. Lin, J. Polym. Res. 6 (1999) 123.
[14] V. Chaturvedi, S. Tanaka, K. Kaeriyama, Macromolecules 25 (1993) 2607.
[15] A. Sakamoto, Y. Furukawa, M. Tasumi, J. Phys. Chem. 96 (1992) 1490.
[16] N.F. Colaneri, D.D.C. Bradley, R.H. Friend, P.L. Burn, A.B. Holmes, C.W. Spangler, Phys. Rev. B 42 (1990) 11670.
[17] D.D.C. Bradley, Synth. Met. 54 (1993) 401.
[18] N.T. Harrison, G.R. Hayes, R.T. Philips, R.H. Friend, Phys. Rev. Lett. 77 (1996) 1881.
[19] I.D.W. Samuel, B. Crystall, G. Rumbles, P.L. Burn, A.B. Holmes, R.H. Friend, Chem. Phys. Lett. 213 (1993) 472.
[20] I.D.W. Samuel, B. Crystall, G. Rumbles, P.L. Burn, A.B. Holmes, R.H. Friend, Synth. Met. 54 (1993) 281.
[21] N.C. Greenham, I.D.W. Samuel, G.R. Hayes, R.T. Philips, Y.A.R.R. Kessener, S.C. Moratti, A.B. Holmes, R.H. Friend, Chem. Phys. Lett. 241 (1995) 89.
[22] L. Smilowitz, A. Hays, A.J. Heeger, G. Wang, J.E. Bowers, J. Chem. Phys. 98 (1993) 6504.
[23] U. Lemmer, R.F. Mahet, Y. Wada, A. Greiner, H. Bässler, E.O. Göbel, Appl. Phys. Lett. 62 (1993) 2827.
[24] M. Yan, L.J. Rothberg, F. Papadimitrakopoulos, M.E. Galvin, T.M. Miller, Phys. Rev. Lett. 73 (1994) 744.
[25] J.R. Lakowicz, Principle of Fluorescence Spectroscopy, Plenum Press, New York, 1983, Chapter 3, p. 52.
[26] J.R. Lakowicz, Principle of Fluorescence Spectroscopy, Plenum Press, New York, 1983, Chapter 10, p. 307.
[27] L.H. Wang, Z.K. Chen, E.T. Kang, H. Meng, W. Haung, Synth. Met. 105 (1999) 85.
[28] J.L. Bredas, R. Silbey, D.S. Boudreux, R.R. Chance, J. Am. Chem. Soc. 105 (1983) 6555.
[29] I.D. Parker, J. Appl. Phys. 75 (1994) 1656.
[30] H. Antoniadis, M.A. Abkowitz, B.R. Hsieh, Appl. Phys. Lett. 65 (1994) 2030.